Life Sciences 229 (2019) 200–209

Contents lists available at ScienceDirect

Life Sciences

journal homepage: www.elsevier.com/locate/lifescie

RAP-8 ameliorates liver fibrosis by modulating cell cycle and oxidative stress

Hongjiao Xu[a], Sihua Hong[a], Zhibin Yan[b], Qian Zhao[a], Ying Shi[b], Nazi Song[a], Junqiu Xie[b,*], Xianxing Jiang[a,*]

[a] School of Pharmaceutical Sciences, Sun Yat-Sen University, 132 East Outer Ring Road, Guangzhou 510006, China
[b] Key Laboratory of Preclinical Study for New Drugs of Gansu Province, School of Basic Medical Sciences, Lanzhou University, Lanzhou 730000, China

ARTICLE INFO

Keywords:
RNA-Seq
RAP-8
Liver fibrosis
Cell cycle
Oxidative stress

ABSTRACT

Aims: The rapeseed protein derived peptide DHNNPQIR (named as RAP-8) has been previously reported to possess antioxidant activity and alleviate liver fibrosis. The purpose of the present study was to investigate the potential crucial pathways involved in ameliorating liver fibrosis of RAP-8.

Main methods: Next-generation sequencing of messenger RNA (RNA-Seq) analysis of the fibrotic and RAP-8 treated mice was performed. Western blot, qPCR and flow cytometry detection analysis were conducted to measure cell cycle and oxidative stress in LX-2 cells and liver samples.

Key findings: 588 overlapped differentially expressed genes were obtained from a batch of genes RAP-8 altered. Gene Ontology enrichment analysis revealed that changes in the most significant modules were mainly enriched in cell division, nuclear division and mitotic cell cycle process, while alterations in Kyoto Encyclopedia of Genes and Genomes were mainly enriched in cell cycle. Thereafter, according to the co-expression network analysis, the regulations of three core genes (Cenpp, Cyp2c55, Serpinh1) were verified that might be targets for treating liver fibrosis. Furthermore, through experimental verification, we demonstrated that RAP-8 induced cell cycle arrest and prevents oxidation stress.

Significance: As a promising therapeutic candidate for hepatic fibrosis treating, RAP-8 exhibited anti-fibrotic effects via exerting cell cycle arrest and inhibiting oxidative stress.

1. Introduction

Hepatic fibrosis is defined as the excessive accumulation of extracellular matrix (ECM), also known as a reversible wound-healing response to liver injury, resulted from a variety of aetiology, including chronic viral infection, autoimmune hepatitis, alcoholic liver disease, and non-alcoholic steatohepatitis [1,2]. Sustained liver damage ultimately results in cirrhosis, which is the end consequence of progressive fibrosis and the most common nonneoplastic cause of mortality worldwide [3,4]. Liver fibrosis also associated with a range of complications, including portal vein thrombosis, development of hepatocellular carcinoma, ascites, and hepatic encephalopathy [5], which represents one of the most common causes of death in adults [6]. However, no treatments have been approved effective and safe for liver fibrosis, revealing the immediate importance to develop therapeutic methods.

As a typical feature of chronic liver disease, oxidative stress is the main contributor in the development of fibrosis [7,8]. Oxidative stress triggers the morphological changes and the activation of hepatic stellate cells (HSCs) [9]. Activated HSCs generate α-smooth muscle actin (α-SMA) positive myofibroblast-like cells, the major source of extracellular matrix (ECM) that continuously forms scar tissue in the fibrotic liver [10]. On the other hand, reactive oxygen species (ROS) and inflammatory response are also linked together [11,12]. HSCs activation was inhibited in NOX1 or NOX4 deficiency mice, the treatment of dual NOX1/4 inhibitor GKT137831 also had the same effects [13,14]. Therefore, a powerful antioxidant sheds new light on impeding the development of liver fibrosis, even cirrhosis.

RAP-8 (sequences: DHNNPQIR) is a natural peptide derived from rapeseed protein and has been reported to show effective in vitro antioxidant activity in human colonic adenocarcinoma cell line Caco-2 [15]. Our previous research has proved that RAP-8 has beneficial actions against nonalcoholic steatohepatitis and related metabolic disorders as well as liver fibrosis in indicated mice models [16]. Anti-inflammatory, anti-oxidative and anti-fibrosis effects were observed in non-alcoholic fatty liver diseases (NAFLD) mice, however, the

* Corresponding authors.
E-mail address: jiangxx5@mail.sysu.edu.cn (X. Jiang).

https://doi.org/10.1016/j.lfs.2019.04.037
Received 6 March 2019; Received in revised form 11 April 2019; Accepted 15 April 2019
Available online 29 April 2019
0024-3205/

mechanisms by which RAP-8 contributes to the amelioration of liver fibrosis are complex and not fully understand.

Properly implement high-throughput, transcriptome-wide analytical technologies have been considered to both precise and accurate when was used in identifying differentially expressed genes (DEGs) in studies of various diseases processes [4]. Based on these distinctive efficacies of RAP-8 against liver fibrogenesis, we performed CCl_4 induced liver fibrosis mice and firstly detected hepatic genome-wide gene expression profile by RNA-Seq analysis for mechanism study. The hub genes predominating with the administration of RAP-8 were investigated by subjecting to gene ontological (GO) analysis and establishing the co-expression networks. The present study may shed new lights on elucidating the role of antioxidative peptide in the inhibition of liver fibrosis and provide more options for treating liver fibrosis in the future.

2. Results

2.1. Differentially expressed genes (DEGs) expression profiles

According to data processing and analysis, we identified a batch of differentially expressed genes among the groups of Oil, CCl_4 and RAP-8. The results of DEGs revealed that 1953 genes met inclusion criteria in CCl_4-induced mice as compared to the Oil-treated mice (Fig. 1a), meanwhile, 1522 genes related mRNAs were differentially expressed in mice with the administration of RAP-8 versus those CCl_4-induced ones (Fig. 1a).

Statistics were performed for the same genes in all three groups, and the Venn Diagram of DEGs was drawn. As shown in Fig. 1b, these analyses intuitively exhibited the number of common and special DEGs is 588 among the different groups. Most of the differentially expressed genes in CCl_4 vs Oil group had the opposite expression patterns in RAP-8 vs CCl_4 group. Then hierarchical clustering of these overlapped genes was performed, as shown in Fig. 2. These results indicated that the genes exhibited distinctly different expression patterns.

2.2. Gene annotation and functional analysis of DEGs

To explore the function and pathways of the 588 identified DEGs, we performed GO and Kyoto Encyclopedia of Genes and Genomes (KEGG) analyses by DAVID. We found that the overlapped genes in the biological processes category were significantly enriched in cell division, mitotic nuclear division and cell cycle (Fig. 3a). Cellular component analysis revealed that most of the common expression genes were located at the proteinaceous extracellular matrix and extracellular region (Fig. 3b). Meanwhile, on the basis of molecular function analysis,

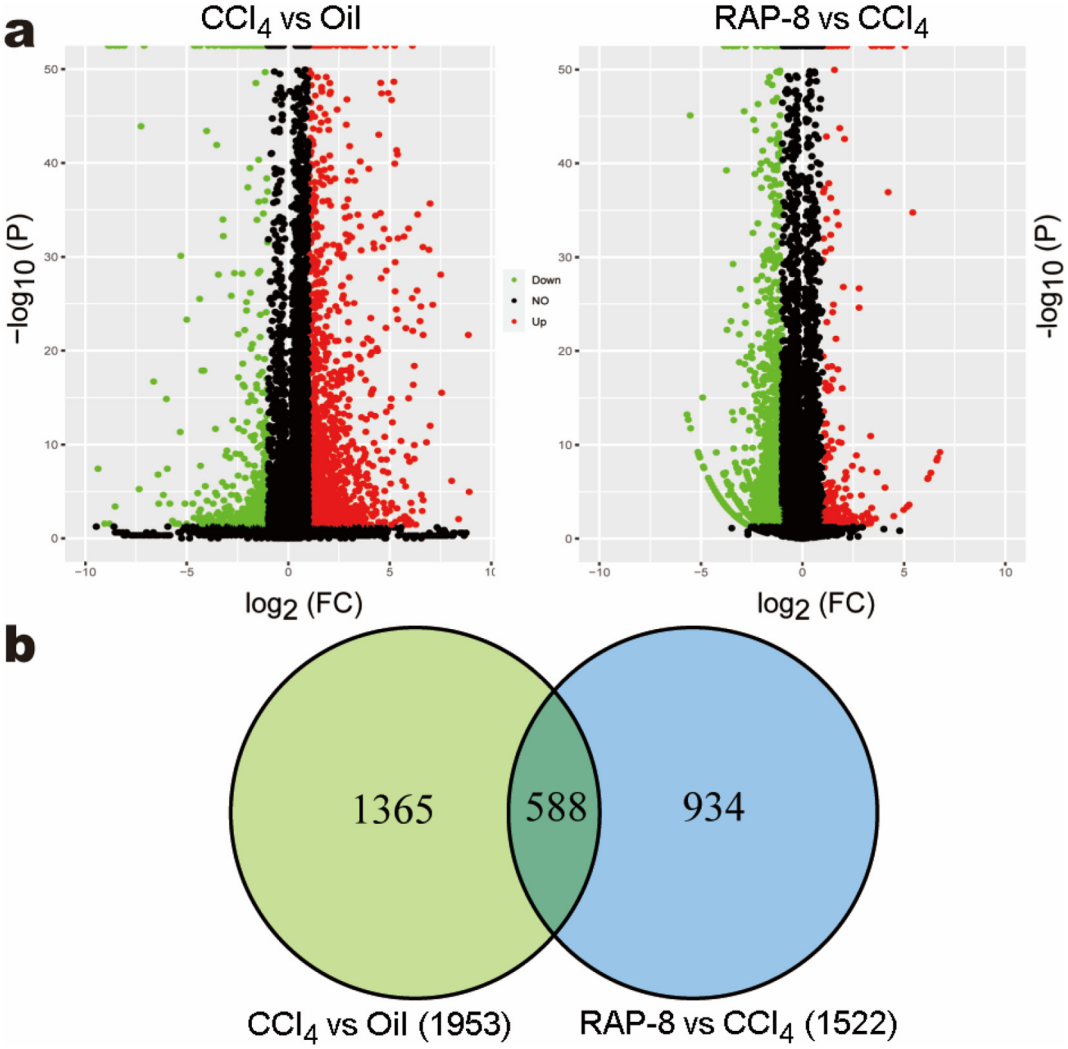

Fig. 1. The expression profiling changes of genes after the administration of RAP-8. (a) Volcano Plot indicated up-regulated and down-regulated genes, which are colored in red and green, respectively. (b) Venn diagram showed the number of overlapped genes is 588. (For interpretation of the references to color in this figure legend, the reader is referred to the web version of this article.)

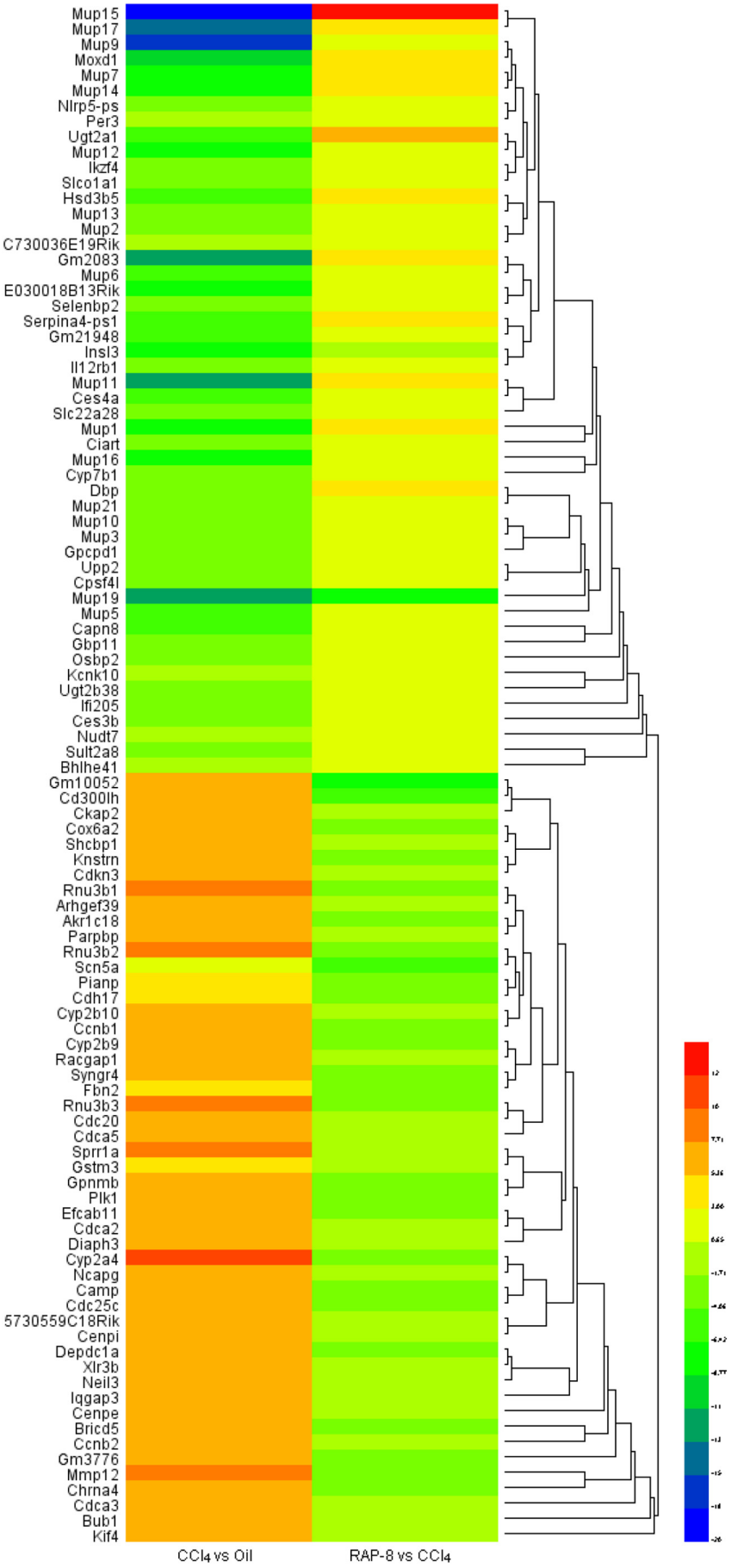

Fig. 2. The clustering heat map for the DEGs. The color brightness is associated with differences in multiples. DEGs: differentially expressed genes.

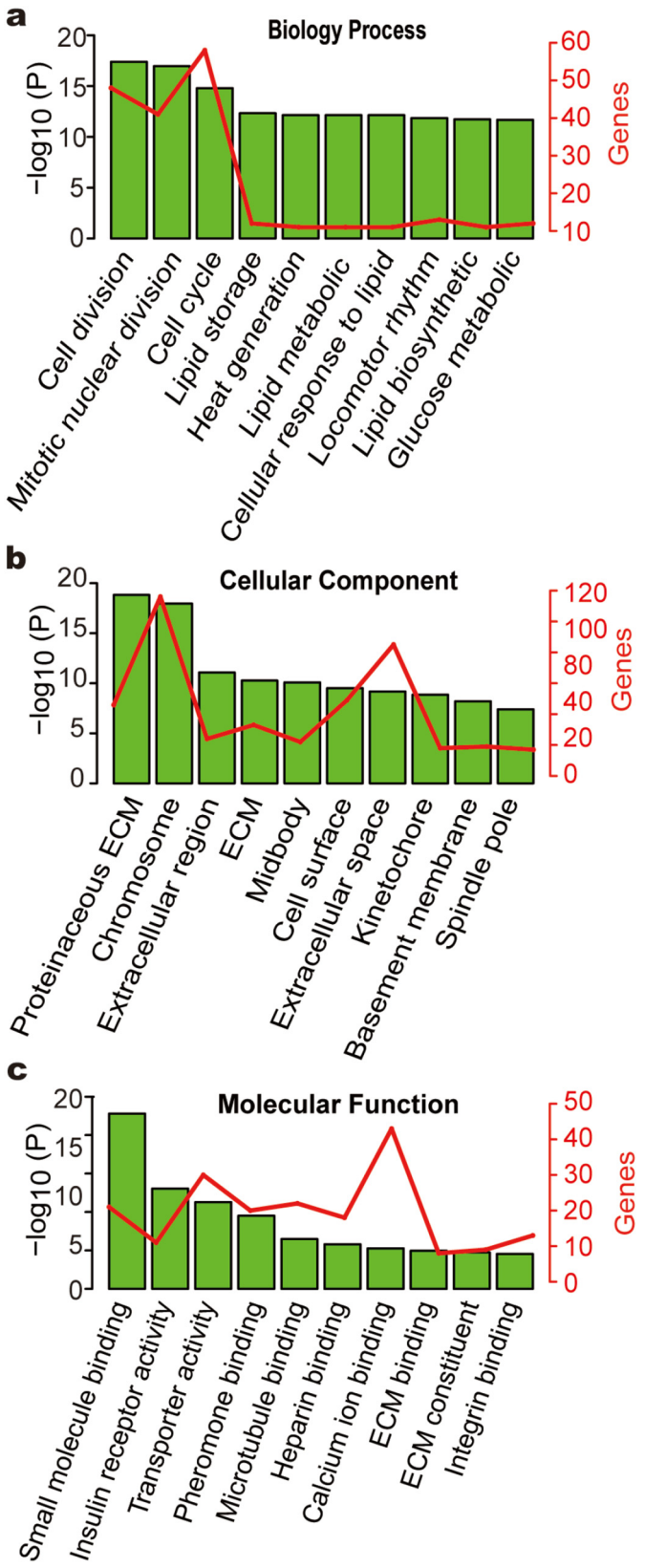

Fig. 3. Top 10 GO enrichment analyses of overlapped DEGs. (a) The functions of the genes involved biological process. (b) The functions of genes related cellular component. (c) The functions of genes involved molecular function. DEGs: differentially expressed genes; GO: Gene Ontology.

these genes were involved in small molecule binding and insulin-activated receptor activity (Fig. 3c). Furthermore, KEGG pathway analysis showed that most of the overlapped genes majorly participated in cell cycle and ECM-receptor interaction (Fig. 4).

2.3. PPI network construction and modules analysis

Protein-protein interaction (PPI) network of the overlapped DEGs was established by Cytoscape based on STRING database. In total, 108 nodes and 297 edges were mapped in the network of identified DEGs (Fig. 5a). Based on centrality parameters of the network (Degree and Betweeness), the 3 highest-scoring modules which represent cell cycle, oxidative stress and ECM accumulation, respectively, were identified from the whole network (Fig. 5b-d). A significant module containing 22 nodes and 221 edges were also generated by the Molecular Complex Detection (MCODE). Hub genes connect most adjacent genes and have the biggest degrees indicated that the connectivity among the nodes was tightly established. As shown in Table 2, Cenpp, Cyp2c55 and Serpinh1 were verified as hub genes. These results suggested that genes in modules were significantly associated with the pathogenesis of liver fibrosis and might be targets for treating liver fibrosis.

2.4. RAP-8 induces cell cycle arrest

According to the results of KEGG pathway analysis, we selected the several genes associate with the cell cycle from overlapped genes and the heat map was showed in Fig. 6a. It was found that expression levels of cell cycle related genes altered by CCl_4 treating were reversed by RAP-8 administration. To further confirm the effects of RAP-8 on cell cycle, the correlative mRNA levels in liver tissues were analyzed by qPCR (Fig. 6b). In accordance with the results of RNA-seq, RAP-8 attenuated the CCl_4 -enhanced levels of cell cycle-related protein. Then, we detected cell-cycle-related proteins in LX-2 cells, including protein cyclin D which facilitates G1/S phase transition, p21, cyclin A and cyclin B which play vital roles in the mitotic spindle dynamics (Fig. 6c). Western blot analysis showed that RAP-8 treatment could downregulate the cyclin A and cyclin B protein expression, and upregulate the expression of p21, a cyclin-dependent kinase (CDK) inhibitor that induced cell cycle arrest [17]. However, RAP-8 did not affect the level of cyclin D1 compared with the control group (Fig. 6d). Whereafter, the influence of RAP-8 on the cell cycle of LX-2 cells was investigated by flow cytometric analysis. As showed in Fig. 6e, compared with control group, cell counts of G2/M phase were significantly elevated in cells treated with RAP-8. These findings imply that RAP-8 reduces liver fibrosis via inducing cell cycle arrest at the G2/M phase.

2.5. RAP-8 attenuates oxidative damage

Increased oxidative stress in liver has been recognized in CCl_4- induced liver fibrosis [18], and ROS was proposed to be crucial for the initiation and development of fibrosis [19]. RAP-8 was already identified as an anti-oxidative peptide [15]. Thus, we investigated whether RAP-8 attenuated liver fibrosis dependent on the inhibition of ROS. NOX4, a professional ROS generator, was tested to explore the effect of RAP-8 on ROS. Immunofluorescence test showed RAP-8 markedly reduced NOX4 expression in CCl_4-induced fibrotic mice (Fig. 7a, b). Meanwhile the mRNA levels of some anti-oxidative genes in the liver tissues were elevated under RAP-8 treatment. Consistent with qPCR results, SOD1 and CAT level were also significantly increased by RAP-8 treatment (Fig. 7c). In addition, the protein expressions levels of NOX1 and NOX4 in LX-2 cells were determined by western blot analysis (Fig. 7d). Data showed that RAP-8 reduced NOX1 and NOX4 protein expression levels (Fig. 7e). Furthermore, RAP-8 treatment significantly attenuated ROS accumulation in LX-2 cells in a dose-dependent manner, indicated by the fluorescent images (Fig. 7f) and microplate reader analysis (Fig. 7g). Taken together, these results showed that

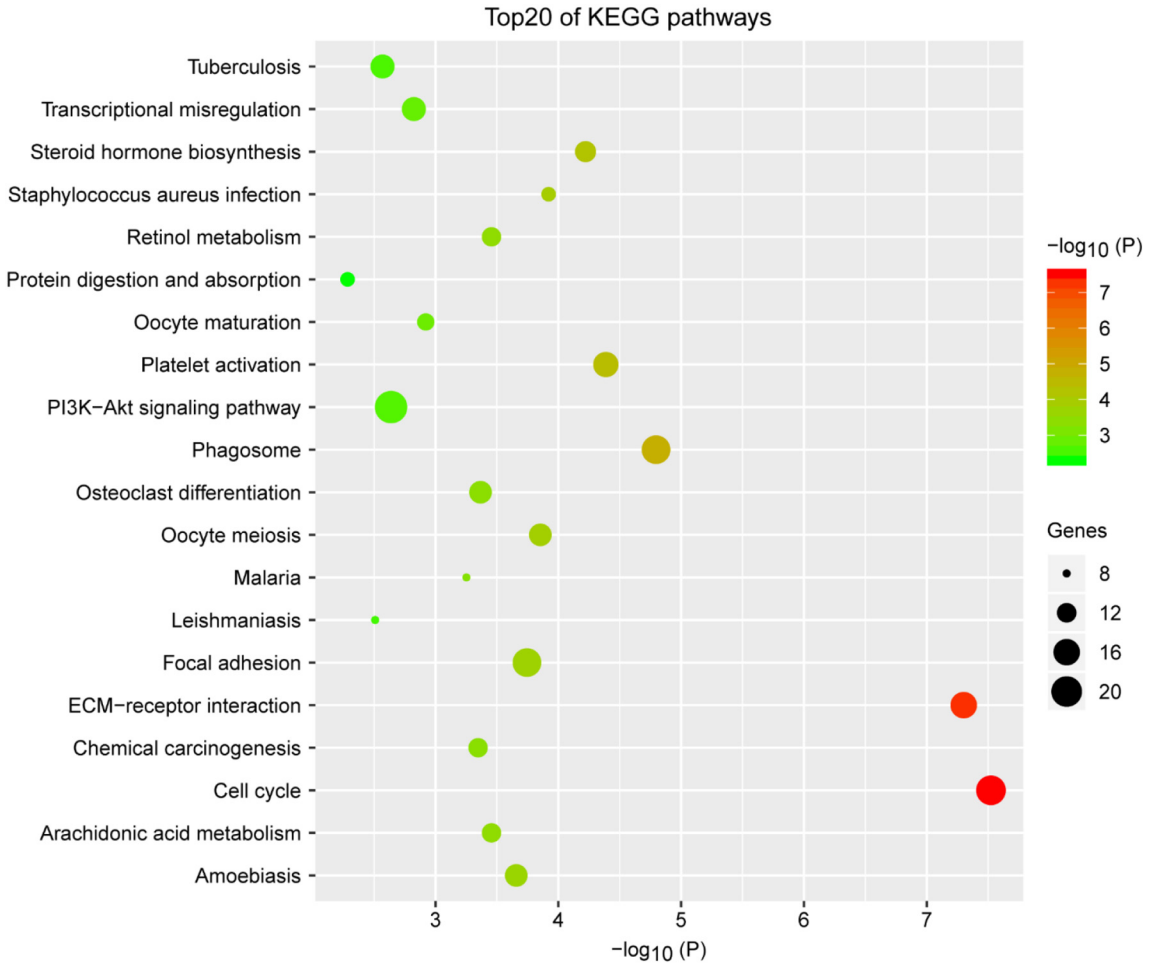

Fig. 4. Top 20 KEGG pathway GO terms enriched for overlapped DEGs. DEGs: differentially expressed genes; GO: Gene Ontology; KEGG: Kyoto Encyclopedia of Genes and Genomes.

RAP-8 ameliorated liver fibrosis via inhibiting oxidative stress.

3. Discussion

Liver fibrosis is a common developmental stage in the majority of chronic liver diseases and may result in liver cirrhosis or the serve end stage liver disease hepatocellular carcinoma (HCC). During the progress of NAFLD, hepatic inflammation and oxidative stress act as the crucial tractive force. Thus, interventions target oxidant stress is considered as effective methods to treat NAFLD. In the previous study, we had assessed the protective effects of RAP-8 on liver injury and hepatic fibrosis. Here in the current study, deploying RNA-seq analysis, we further investigated the possible mechanism of RAP-8 in protecting against liver fibrosis by screening a series of altered expressed genes. By using the combination of gene annotation, GO, KEGG pathways and PPI network analysis, we demonstrated that the identified DEGs associated with fibrosis were related to cell cycle and oxidative stress. Additionally, these results were validated through a batch of experiments.

To be specific, the current researches were designed based on the identified DEGs that may be involved in liver fibrosis. A total of 588 DEGs and 3 hub genes were identified and might be regarded as biomarkers for liver fibrosis. The present study further demonstrated the mechanism for RAP-8-mediated protection against liver fibrosis in vitro and in vivo. Although RAP-8 has previously been demonstrated its mediated protection against liver fibrosis by apoptosis [16], the effects on cell cycle had not been studied yet. According to our results, as a promising new treatment of liver fibrosis, RAP-8 might play its role through the inhibition of oxidative stress and the mediation of cell cycle. However, further exploration and research are needed to elucidate the biological function of these hub genes in the progress of liver fibrosis.

Oxidative stress has been implicated in the pathogenesis of liver fibrosis. Major sources of ROS are NAD(P)H oxidases, a multi-component complex that catalyzes reactions from molecular oxygen to ROS [22]. Elevated levels of ROS produced by oxidative stress is an important stimulant in the activation process of hepatic stellate cells (HSCs) [21]. Therefore, activated HSCs need to harbor highly effective anti-oxidants to protect against the toxic effects of ROS [23]. Since oxidative stress results from an imbalance between oxidants and antioxidants, a number of antioxidants are necessary to counteract harmful effects [20]. Moreover, numerous studies had demonstrated the role of antioxidants in preventing liver fibrosis [13,24,25]. In previous research, RAP-8 has been known to act as an antioxidant/free radical scavenger or reducing agent. The administration of RAP-8 has been reported to reduce oxidative stress in HFD-induced NASH mice [15,16]. In this study, with the administration of RAP-8, NOX1 and NOX4 expression levels were decreased, the liver sod and cat levels were increased, signifying the counteracting role of RAP-8 against the oxidative stress induced by CCl_4. In addition, RAP-8 reduced the production of ROS in LX-2 cells. Further studies based on an animal model more closely resembling human liver fibrosis may be helpful to evaluate the applicability of RAP-8.

Cell cycle progression is operated by cyclin and cyclin-dependent

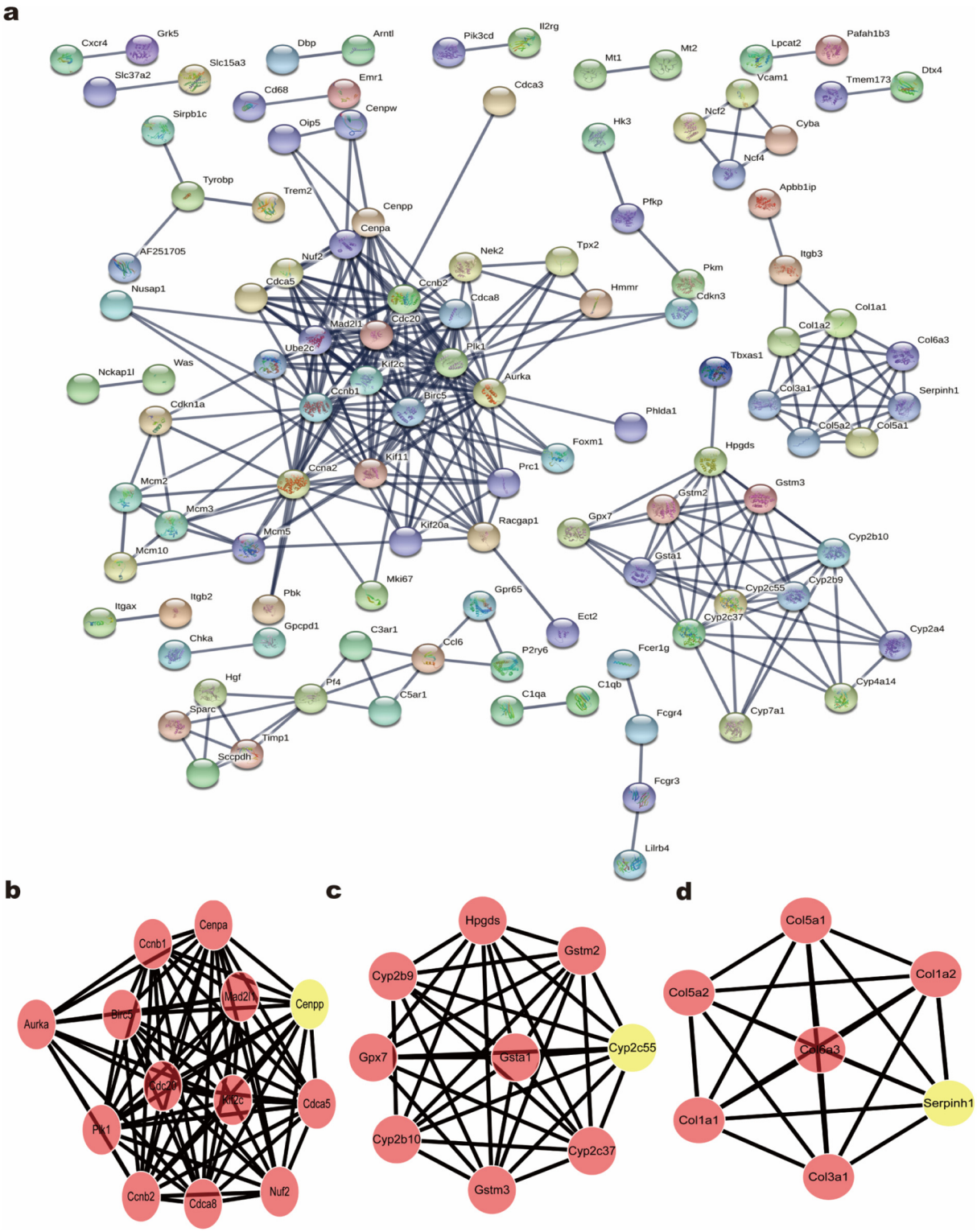

Fig. 5. Establishment of PPI network and modules analysis for overlapped DEGs. (a) Entire PPI network. (b) PPI network of module 1. (c) PPI network of module 2. (d) PPI network of module 3. PPI: protein–protein interaction. DEGs: differentially expressed genes.

kinase(CDK) complexes [26]. Cyclin D1/CDK4 and Cyclin E/CDK2 complexes perform important roles in promoting the transition from the G0/G1 to the S phase [27]. Cyclin A and Cyclin B are mainly expressed during the G2/M phase [28]. Liver fibrogenesis involves cell cycle re-entry of quiescent cells such as hepatocytes and HSCs. Previous studies have reported that dysregulation of the cell cycle process and mitotic cell cycle played important roles in the development of liver fibrosis, although few studies on cell cycle in liver fibrosis have been performed [29]. The anti-proliferative effect of silibinin on human stellate cell line LX-2 is via the inhibition of the expressions of various cell cycle targets including p27, AKT and sirtuin signaling [30]. Christian and co-workers have suggested that the inhibition of Cyclin E1 prevented progression of CCl_4-induced liver fibrosis by RNA interference [31]. Recently, Chen et al described that with exposing to soluble egg antigens from

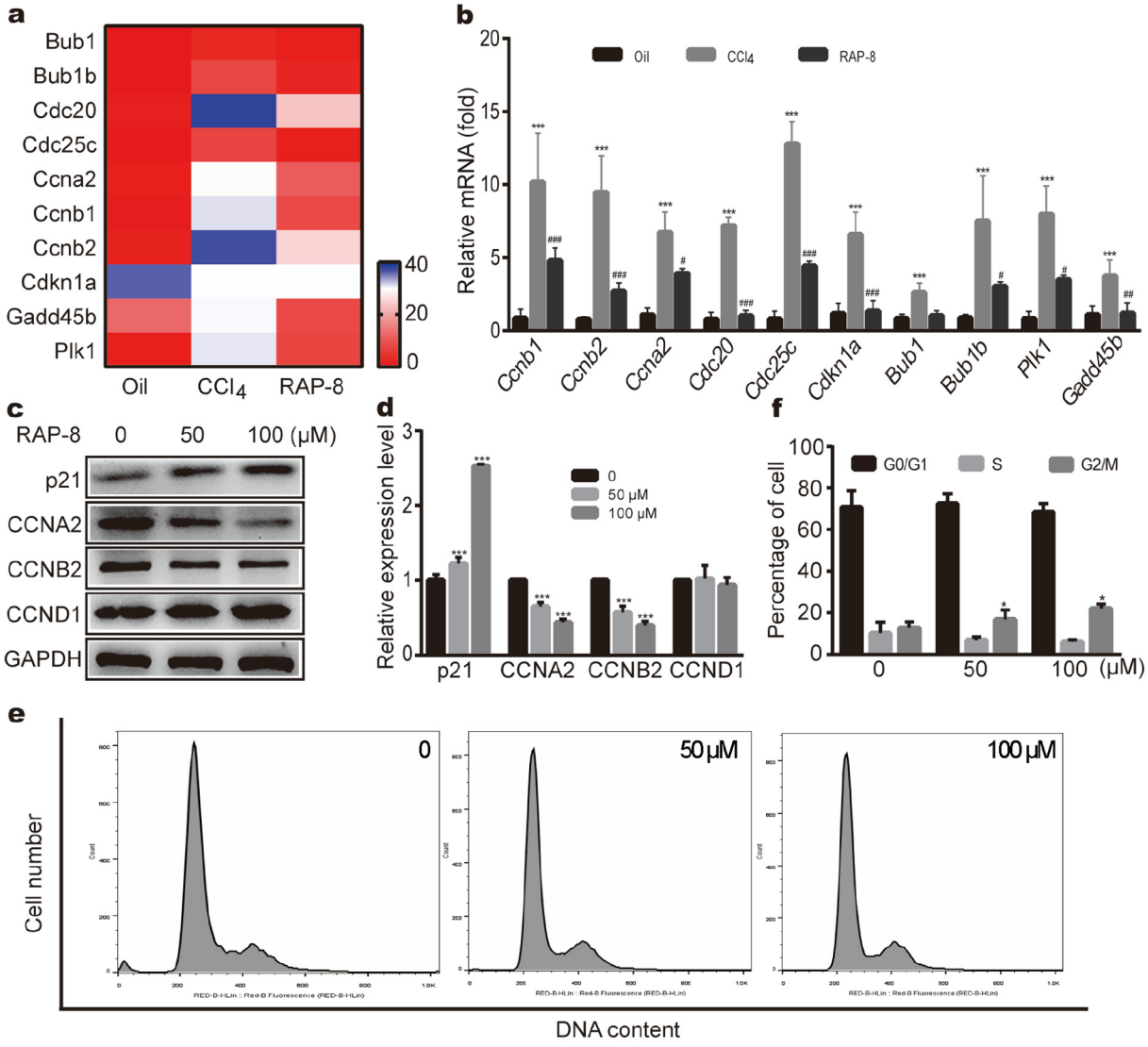

Fig. 6. Effects of RAP-8 on cell cycle. (a) RNA-seq analysis of genes involved in cell cycle (P (Probability value) $<$ 0.01, | FC (fold change) | $>$ 2); (b) qPCR analysis of genes involved in cell cycle; (c) Western blot analysis for p21, CCNA2, CCNB2 and CCND1 in LX-2 cells; (d) Densitometric analysis of the blots shown in c. (e, f) Flow cytometry analysis of the DNA content of LX-2 cells under the administration of RAP-8. * and ** denote significant differences ($P < 0.05$ and $P < 0.01$, respectively) from the Oil group; ## denotes significant differences ($P < 0.01$) from the CCl_4-induced group.

Schistosoma japonicum, activated HSCs exhibited cell cycle arrest with an increased expression level of P-p53 and p21. Notably, the authors found that a novel STAT3-p53-p21 pathway might participate in the senescence of HSCs [32]. Our previous studies have showed that RAP-8 exhibited potent anti-fibrosis activity against CCl_4-induced mouse model by inhibiting apoptosis [16]. The molecular mechanisms behind the cell cycle arrest by RAP-8 in liver fibrosis remain largely unclear. Here, through RNA-seq and experimental analysis, we showed for the first time that RAP-8 treatment reduces liver fibrosis via causing G2/M arrest and decreasing expression of Cyclin A1 and Cyclin B1 (Fig. 5). These results obtained herein are in agreement with other reports which demonstrated that RAP-8 induced cell cycle arrest and apoptosis in Caco-2 cells [15]. Still, we need to further investigate how RAP-8 contributes to the inhibition of cell cycle mediators such as cell cycle dependent kinases and cyclins.

4. Conclusion

In conclusion, our results demonstrated for the first time that RAP-8 blocks liver fibrosis through the inhibition of oxidative stress and cell cycle arrest. These results indicated a new anti-fibrotic mechanism of RAP-8 and provided a new treatment of liver fibrosis in a variety of chronic liver diseases.

5. Materials and methods

5.1. Reagents

Dulbecco's modified eagle's medium (DMEM) was from Gibco Invitrogen Corporation (Carlsbad, CA). Fetal bovine serum (FBS), Penicillin/streptomycin solution, 0.05% Trypsin-EDTA and phosphate-buffered saline (PBS) were purchased from Thermo Fisher Scientific (USA). Dimethyl sulfoxide (DMSO), and 2′,7′-dichlorodihydro-fluorescein diacetate were obtained from Sigma (St. Louis, MO, USA). Antibodies were obtained from the following sources: anti-CCNB (1:1000), anti-CCNA (1:1000), and anti-CCND (1:1000) antibody were from Abcam (Cambridge, UK); p21 (1:1000), anti-NOX4 (1:500) and anti-NOX1 (1:500) were from BOSTER (California, US); Anti-rabbit IgG (H + L) antibody (1:10000) was from Cell Signaling Technology, Inc. (Beverly, MA, USA); anti-GAPDH mAb (1:5000), horseradish peroxidase (HRP)-conjugated AffiniPure goat anti-mouse IgG and anti-rabbit IgG were purchased from Zhongshan Golden Bridge Biotechnology Co,

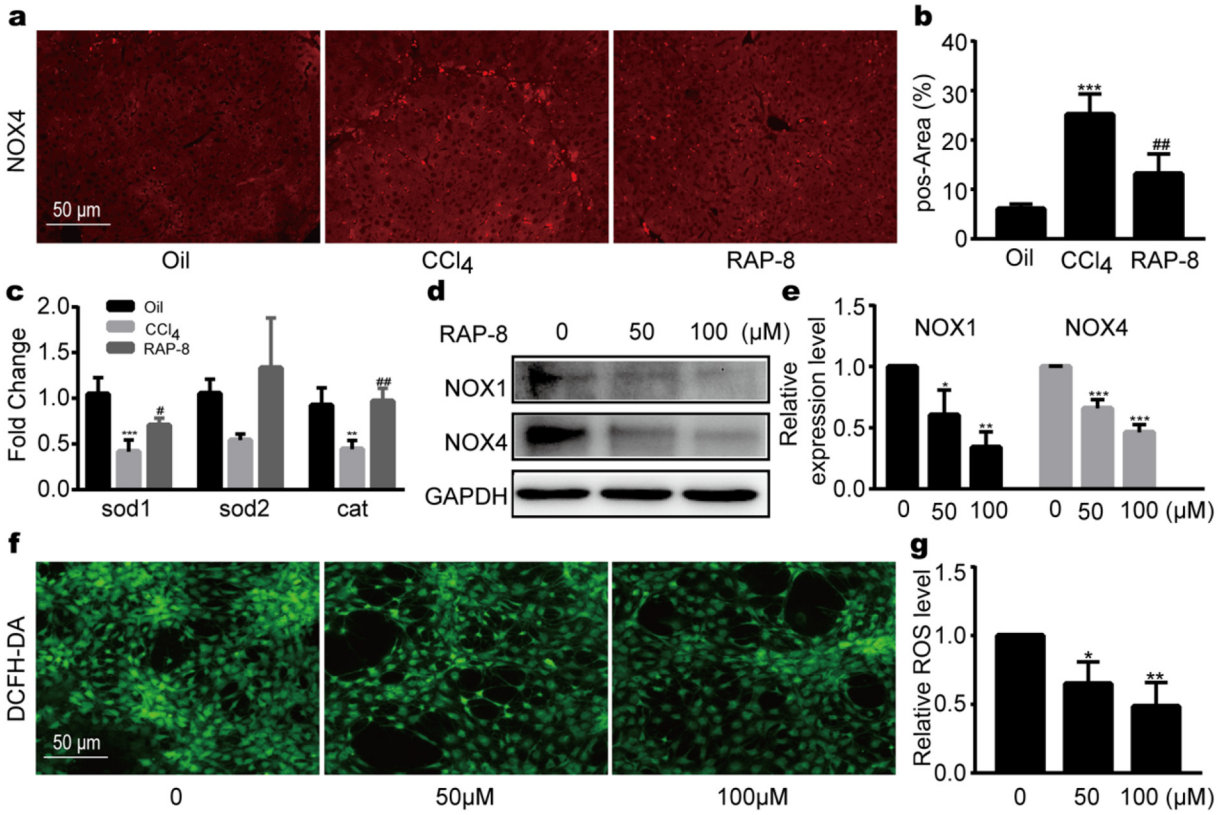

Fig. 7. The reduction of oxidative stress was responsible for anti-fibrotic effect of RAP-8. (a) NOX4 expression was decreased with the treatment of RAP-8. (b) Quantification of the NOX4 expression in the indicated groups. (c) RAP-8 treatment increased antioxidative gene level. (d) RAP-8 suppressed the expression of NOX1/NOX4 in LX-2 cells. (e) Densitometric analysis of the blots shown in d. Intracellular ROS content was determined by fluorescent images (f) and microplate reader (g). $^{*}P < 0.05$ and $^{**}P < 0.01$, CCl_4-induced group vs Oil group; ## $P < 0.01$, RAP-8 treated group vs CCl_4-induced group.

Ltd. (Beijing, China). Enhanced chemiluminescence (ECL) substrate for detection of HRP were obtained from Bio-Rad. The peptide RAP-8 (DHNNPQIR) was obtained as previously described [16].

5.2. Animals and treatment

Six-week-old male C57BL/6J mice were used and purchased from the Experimental Animal Center of Sun Yat-sen University in the study. Mice were kept under a 12-h light/dark cycles, the temperature was kept at 25 ± 1 °C, and fed with regular experimental rodent forage provided by Experimental Animal Center of Sun Yat-sen University and clean water ad libitum. The animals had free access to food and tap water. All experimental protocols and animal husbandry were conducted in accordance with the guidelines of the Care and Use of Laboratory Animals, as adopted and promulgated by the U.S. National Institutes of Health Animal Care, and all studies were approved by the Laboratory Animals Use Committee of the Sun Yat-sen University.

The methods of RAP-8 administration on hepatic fibrosis were carried out as we previously described [16]. Liver fibrosis was induced by intraperitoneally (i.p) injection with CCl_4 (diluted at 1:4 in corn oil) (5 ml/kg body weight) twice a week for 6 weeks. Control mice were injected with corn oil alone at the equivalent volume and frequency. The treatment groups were injected intraperitoneally with RAP-8 (500 μg/kg) since the 4th week. All animals were euthanized at week 7 under ether anesthesia. Blood and livers were collected, and the liver samples were fixed in formalin.

5.3. RNA-Seq data analysis and identification of DEGs

The differential expression analysis among three groups (seven biological replicates per group) was analyzed using DESeq. *P*-value of < 0.01 and |foldchange value| ≥ 2 were set as the screening criterion for DEGs.

5.4. Gene Ontology and pathway enrichment analysis of DEGs

GO consists of three items: molecular functions, biological processes and cellular components. The Kyoto Encyclopedia of Genes and Genomes (KEGG) is a set of high-throughput genes and protein pathways. The GO and KEGG analyses of DEGs were performed in the DAVID 6.8 (https://david.ncifcrf.gov/), which is a bioinformatics database containing three parts: Molecular Functions (MF), Cellular Components(CC) and Biological Processes (BP) that aiming at uncovering perturbed biological processes [33,34].

5.5. Protein–protein interaction (PPI) network and module analysis

The comprehensive interactions of the DEGs from which we obtained was assembled and evaluated by using The Search Tool for the Retrieval of Interacting Genes (STRING) database (http://string-db.org/). The PPI network was visualized using Cytoscape v 2.8.3 software, which is an open-source tool for network visualization of proteins, genes and other types of biological molecules. In short, DEGs were uploaded to STRING to build a PPI network and then visualized using Cytoscape. The cut-off criteria of the extended network that we constructed are a high confidence score > 0.9 for a PPI network and a node degree of > 10 for screening hub genes. Then a Cytoscape plug-in "The Molecular Complex Detection (MCODE)" was used to screen modules of hub genes from the PPI network. In the network, nodes represent proteins and edges represent interactions between two proteins.

Table 1
Primer sequences used for semi-quantitative RT-PCR analysis.

Gene	Primer sequence (5′-3′)
Bub1-F	AGAATGCTCTGTCAGCTCATCT
Bub1-R	TGTCTTCACTAACCCACTGCT
Bub1b-F	GAGGCGAGTGAAGCCATGT
Bub1b-R	TCCAGAGTAAAAGCGGATTTCAG
Cdc20-F	GGAGGTGACCGCTTTATCCC
Cdc20-R	CCAGGCTTTCTGATGCTCCT
Cdc25c-F	ATGTCTACAGGACCTATCCCAC
Cdc25c-R	ACCTAAAACTGGGTGCTGAAAC
Ccna2-F	GCCTTCACCATTCATGTGGAT
Ccna2-R	TTGCTCCGGGTAAAGAGACAG
Ccnb1-F	CTTGCAGTGAGTGACGTAGAC
Ccnb1-R	CCAGTTGTCGGAGATAAGCATAG
Ccnb2-F	GCCAAGAGCCATGTGACTATC
Ccnb2-R	CAGAGCTGGTACTTTGGTGTTC
Cdkn1a-F	CCTGGTGATGTCCGACCTG
Cdkn1a-R	CCATGAGCGCATCGCAATC
Gadd45b-F	CAACGCGGTTCAGAAGATGC
Gadd45b-R	GGTCCACATTCATCAGTTTGGC
Mcm2-F	ATCCACCACCGCTTCAAGAAC
Mcm2-R	TACCACCAAACTCTCACGGTT
Plk1-F	CTTCGCCAAATGCTTCGAGAT
Plk1-R	TAGGCTGCGGTGAATTGAGAT
Sod1-F	AACCAGTTGTGTTGTCAGGAC
Sod1-R	CCACCATGTTTCTTAGAGTGAGG
Sod2-F	CAGACCTGCCTTACGACTATGG
Sod2-R	CTCGGTGGCGTTGAGATTGTT
Cat-F	AGCGACCAGATGAAGCAGTG
Cat-R	TCCGCTCTCTGTCAAAGTGTG
Gapdh-F	AGGTCGGTGTGAACGGATTTG
Gapdh-R	TGTAGACCATGTAGTTGAGGTCA

5.6. RNA extraction and qPCR

Liver tissues of all groups were homogenized with homogenizer. Then, total RNA was extracted with Trizol Reagent (Invitrogen, Carlsbad, CA) and RNA quality was assessed with Agilent 2100 Bioanalyzer (Agilent Technologies, Santa Clara, CA). For cDNA synthesis, 1 μg isolated total RNA subjected to reverse transcription with a High-Capacity cDNA Reverse Transcriptase Kit (TransGen Biotech, China) on a LightCycler 480 System II (Roche Applied Science, Indianapolis, IN, USA).Subsequently, cDNA was amplified by Quantitative real-time polymerase chain reaction using a SYBR Green I PCR Master Kit (TransGen Biotech, China) on a Step One instrument (Applied Biosystems) as follows: denaturation at 95 °C for 1 min followed by 40 cycles of 15 s at 95 °C and extension at 55 °C for 30 s. A melting curve of each amplicon was determined to verify its accuracy. The primer sequences are listed in Table 1. The levels of target Genes were normalized to GAPDH as an internal reference.

5.7. Cell culture

Human hepatic activated stellate cell line LX2 which we used in this study was obtained from Type Culture Collection of the Chinese Academy of Sciences (Shanghai, China). Cells were cultured in DMEM supplied with 10% FBS and 1% penicillin/streptomycin solution in a humidified atmosphere of 5% CO_2 at 37 °C. LX2 cells were seeded in a 6-well or 96-well plate, for different purposes, and then the adherent cells were exposed to indicated concentrations of RAP-8 for another 48 h. After that, the cells were obtained for different experiments.

Table 2
The three highest-scoring modules were identified from the whole network.

Cluster	Score	Seed gene	Nodes	Edges
Cluster 1	12.500	Cenpp	13	75
Cluster 2	8.500	Cyp2c55	9	34
Cluster 3	7.000	Serpinh1	7	21

5.8. Western blot assay

Liver tissue samples were homogenized with Automated Tissue Homogenization (JXFSTPRP-24, JinXin, Shanghai). Total protein from liver tissues of all groups was obtained in this way were dissolved in RIPA lysis buffer (50 mM Tris-HCl (pH 8.0), 150 mM NaCl, 0.02% w/v NaN3, 0.1% w/v SDS, 1% *v*/v NP-40, 0.5% w/v Sodium deoxycholate, 1 mM EDTA, and 1 mM PMSF; BBI Life Sciences.). The LX-2 cells were washed two times with phosphate buffered saline (PBS) prior to collection. RIPA buffer was added to collected cells on the ice for 30 min, and centrifuged for 30 min at 12,000*g* to obtain supernatants. Electrophoresis was performed on a 12% SDS–polyacrylamide gel. Electrophoresed proteins were transferred to 0.45 μm PVDF membranes (Immobilon -PSQtransfer membranes, Merck Millipore, Germany) for 1.5 h at 250 mA, and the blotted membrane were then blocked with 5% skim milk for 1 h at room temperature. The membranes then were incubated with the antibodies overnight at 4 °C. The membranes were then fixed with horse-radish peroxidase (HRP) conjugated anti-mouse/rabbit IgG (Promega) for 1 h and the immobilized proteins were detected by enhanced chemoluminescence (ECL). The densitometric measurement of each band was analyzed using Quantity-One Protein Analysis Software (Bio-Rad, Hercules, CA, United States). Equal loading of proteins was verified by immunoblotting for GAPDH.

5.9. Flow cytometric analysis

Cell cycle analysis was detected by propidium iodide staining. In briefly, the LX2 cells were plated in 6-well plates at a density of 5×10^4 cells per well for 24 h. After another 48 h treatment of RAP-8 (0, 50 and 100 μM), the cells were harvested and fixed in ice-cold 70% ethanol overnight at 4 °C. Fixed cells were washed with cooled PBS and stained using the cell cycle assay kit (Bestbio, BB-4104). The DNA content was analyzed by flow cytometry (FACSCalibur; Becton Dickinson), and percentages of cells in G0/G1, S and G2/M cell-cycle phases were performed using FlowJo software (Tree Star). At least 10,000 nuclei were counted for each sample.

5.10. Immunofluorescence

Liver samples fixed in 10% buffered formalin were embedded in paraffin blocks, then sectioned, deparaffinized and rehydrated. Liver sections (4 μm thick) were processed using a standard immunostaining protocol. In brief, 3% H_2O_2 was used to block endogenous peroxidase after antigen retrieval in citrate buffer (pH = 6.0) that performed in a microwave oven for 15 min, and the slides were then blocked with 5% BSA/PBS solution. For immunofluorescent staining, the mouse liver sections were incubated with the primary antibody against NOX4 (1:200, BOSTER, Wuhan) overnight at 4 °C and then Alexa Fluor 594-conjugated secondary antibodies (1:200, Zhongshan Golden Bridge Biotechnology) for 1 h at 37 °C. Finally, the slides were viewed and photographed under the fluorescent microscopy. The area of positive staining was measured in highpower (X20) fields on each slide and quantified using Image J software.

5.11. Reactive oxygen species (ROS) determination in LX-2 cells

A fluorescent probe, DCFH-DA, was used for determination of intracellular ROS levels. LX-2 cells were seeded into 96-well black plates for 24 h. Cells were washed with 1 × PBS twice, pretreated with different concentrations of RAP-8 or DMEM for 24 h. After RAP-8 treatment followed with 15 min, the cells were incubated with 2′,7′-dichlorodihydrofluorescein diacetate (10 μM) (Sigma Aldrich). Then cells were washed with PBS for three times and incubated with DCFH-DA (10 μM) at 37 °C for 15 min. Subsequently, the intracellular fluorescent

intensity was determined by a FlexStation 3 Multi-Mode Microplate Reader with the excitation and emission wavelengths at 485 and 535 nm, respectively. Meanwhile, an ArrayScanVTI was used to observe the intracellular fluorescence.

5.12. Statistical analysis

Values were expressed as mean ± SD. Statistical differences between two groups were analyzed by the unpaired Student's *t*-test and differences between multiple groups of data were analyzed by one-way ANOVA with Bonferroni correction (GraphPad Prism 7.0, San Diego, CA, USA). A $P < 0.05$ was considered statistically significant.

Conflicts of interest

There are no conflicts to declare.

Author contributions

X.J. and J.X. conceived and designed the research and supervised the studies. H.X., Z.Y. performed the experiments and analyzed data. Q.Z., N.Z. and Y·S performed the animal experiments and the acquisition of data. H.X. and Z.Y. analyzed the data and wrote the manuscript.

Acknowledgements

We appreciate the financial support from the National Natural Science Foundation of China (Nos. 91853106, 81602945), and the Program for Guangdong Introducing Innovative and Enterpre-neurial Teams (No. 2016ZT06Y337).

References

[1] E.L. Ellis, D.A. Mann, Clinical evidence for the regression of liver fibrosis, J. Hepatol. 56 (5) (2012) 1171–1180.
[2] T. Tsuchida, S.L. Friedman, Mechanisms of hepatic stellate cell activation, Nat. Rev. Gastroenterol. Hepatol. 14 (7) (2017) 397–411.
[3] V. Hernandez-Gea, S.L. Friedman, Pathogenesis of liver fibrosis, Annu. Rev. Pathol. 6 (2011) 425–456.
[4] Y.Y. Lu, Q.L. Chen, Y. Guan, Z.Z. Guo, H. Zhang, W. Zhang, et al., Transcriptional profiling and co-expression network analysis identifies potential biomarkers to differentiate chronic hepatitis B and the caused cirrhosis, Mol. BioSyst. 10 (5) (2014) 1117–1125.
[5] L. Petitclerc, G. Sebastiani, G. Gilbert, G. Cloutier, A. Tang, Liver fibrosis: review of current imaging and MRI quantification techniques, J. Magn. Reson. Imaging 45 (5) (2017) 1276–1295.
[6] H. Rehman, Q. Liu, Y. Krishnasamy, Z. Shi, V.K. Ramshesh, K. Haque, et al., The mitochondria-targeted antioxidant MitoQ attenuates liver fibrosis in mice, Int. J. Physiol. Pathophysiol. Pharmacol. 8 (1) (2016) 14–27.
[7] J.E. Puche, Y. Saiman, S.L. Friedman, Hepatic stellate cells and liver fibrosis, Compr. Physiol. 3 (4) (2013) 1473–1492.
[8] V. Sanchez-Valle, N.C. Chavez-Tapia, M. Uribe, N. Mendez-Sanchez, Role of oxidative stress and molecular changes in liver fibrosis: a review, Curr. Med. Chem. 19 (28) (2012) 4850–4860.
[9] E. Novo, C. Busletta, L.V. Bonzo, D. Povero, C. Paternostro, K. Mareschi, et al., Intracellular reactive oxygen species are required for directional migration of resident and bone marrow-derived hepatic pro-fibrogenic cells, J. Hepatol. 54 (5) (2011) 964–974.
[10] Y.W. Chiu, P.Y. Chao, C.C. Tsai, H.L. Chiou, Y.C. Liu, C.C. Hung, et al., Ocimum gratissimum is effective in prevention against liver fibrosis in vivo and in vitro, Am. J. Chin. Med. 42 (4) (2014) 833–852.
[11] X. Zhang, J.H. Zhang, X.Y. Chen, Q.H. Hu, M.X. Wang, R. Jin, et al., Reactive oxygen species-induced TXNIP drives fructose-mediated hepatic inflammation and lipid accumulation through NLRP3 inflammasome activation, Antioxid. Redox Signal. 22 (10) (2015) 848–870.
[12] H. Jaeschke, Reactive oxygen and mechanisms of inflammatory liver injury: present concepts, J. Gastroenterol. Hepatol. 26 (Suppl. 1) (2011) 173–179.
[13] T. Aoyama, Y.H. Paik, S. Watanabe, B. Laleu, F. Gaggini, L. Fioraso-Cartier, et al., Nicotinamide adenine dinucleotide phosphate oxidase in experimental liver fibrosis: GKT137831 as a novel potential therapeutic agent, Hepatology 56 (6) (2012) 2316–2327.
[14] T. Lan, T. Kisseleva, D.A. Brenner, Deficiency of NOX1 or NOX4 prevents liver inflammation and fibrosis in mice through inhibition of hepatic stellate cell activation, PLoS One 10 (7) (2015) e0129743.
[15] F. Xu, L. Wang, X. Ju, J. Zhang, S. Yin, J. Shi, et al., Transepithelial transport of YWDHNNPQIR and its metabolic fate with cytoprotection against oxidative stress in human intestinal Caco-2 cells, J. Agric. Food Chem. 65 (10) (2017) 2056–2065.
[16] Q. Zhao, H. Xu, S. Hong, N. Song, J. Xie, Z. Yan, et al., Rapeseed protein-derived antioxidant peptide RAP ameliorates nonalcoholic steatohepatitis and related metabolic disorders in mice, Mol. Pharm. 16 (2018) 371–381.
[17] A. Karimian, Y. Ahmadi, B. Yousefi, Multiple functions of p21 in cell cycle, apoptosis and transcriptional regulation after DNA damage, DNA Repair 42 (2016) 63–71.
[18] X. Huang, X. Wang, Y. Lv, L. Xu, J. Lin, Y. Diao, Protection effect of kallistatin on carbon tetrachloride-induced liver fibrosis in rats via antioxidative stress, PLoS One 9 (2) (2014) e88498.
[19] F. Zhou, A. Wang, D. Li, Y. Wang, L. Lin, Pinocembrin from Penthorum chinense Pursh suppresses hepatic stellate cells activation through a unified SIRT3-TGF-beta-Smad signaling pathway, Toxicol. Appl. Pharmacol. 341 (2018) 38–50.
[20] S. Le Lay, G. Simard, M.C. Martinez, R. Andriantsitohaina, Oxidative stress and metabolic pathologies: from an adipocentric point of view, Oxidative Med. Cell. Longev. 2014 (2014) 908539.
[21] G. Svegliati Baroni, L. D'Ambrosio, G. Ferretti, A. Casini, A. Di Sario, R. Salzano, et al., Fibrogenic effect of oxidative stress on rat hepatic stellate cells, Hepatology 27 (3) (1998) 720–726.
[22] L.L. Hilenski, R.E. Clempus, M.T. Quinn, J.D. Lambeth, K.K. Griendling, Distinct subcellular localizations of Nox1 and Nox4 in vascular smooth muscle cells, Arterioscler. Thromb. Vasc. Biol. 24 (4) (2004) 677–683.
[23] S. Dunning, A. Ur Rehman, M.H. Tiebosch, R.A. Hannivoort, F.W. Haijer, J. Woudenberg, et al., Glutathione and antioxidant enzymes serve complementary roles in protecting activated hepatic stellate cells against hydrogen peroxide-induced cell death, Biochim. Biophys. Acta 1832 (12) (2013) 2027–2034.
[24] M. Di Pascoli, M. Divi, A. Rodriguez-Vilarrupla, E. Rosado, J. Gracia-Sancho, M. Vilaseca, et al., Resveratrol improves intrahepatic endothelial dysfunction and reduces hepatic fibrosis and portal pressure in cirrhotic rats, J. Hepatol. 58 (5) (2013) 904–910.
[25] E. Mormone, Y. Lu, X. Ge, M.I. Fiel, N. Nieto, Fibromodulin, an oxidative stress-sensitive proteoglycan, regulates the fibrogenic response to liver injury in mice, Gastroenterology 142 (3) (2012) 612–621 (e5).
[26] F. Zhang, D.S. Kong, Z.L. Zhang, N. Lei, X.J. Zhu, X.P. Zhang, et al., Tetramethylpyrazine induces G0/G1 cell cycle arrest and stimulates mitochondrial-mediated and caspase-dependent apoptosis through modulating ERK/p53 signaling in hepatic stellate cells in vitro, Apoptosis: an international journal on programmed cell death 18 (2) (2013) 135–149.
[27] Y. Peng, H. Yang, N. Wang, Y. Ouyang, Y. Yi, L. Liao, et al., Fluorofenidone attenuates hepatic fibrosis by suppressing the proliferation and activation of hepatic stellate cells, Am. J. Physiol. Gastrointest. Liver Physiol. 306 (3) (2014) G253–G263.
[28] N. Bendris, B. Lemmers, J.M. Blanchard, Cell cycle, cytoskeleton dynamics and beyond: the many functions of cyclins and CDK inhibitors, Cell Cycle 14 (12) (2015) 1786–1798.
[29] Y.A. Nevzorova, J.M. Bangen, W. Hu, U. Haas, R. Weiskirchen, N. Gassler, et al., Cyclin E1 controls proliferation of hepatic stellate cells and is essential for liver fibrogenesis in mice, Hepatology 56 (3) (2012) 1140–1149.
[30] D. Ezhilarasan, J. Evraerts, B. Sid, P.B. Calderon, S. Karthikeyan, E. Sokal, et al., Silibinin induces hepatic stellate cell cycle arrest via enhancing p53/p27 and inhibiting Akt downstream signaling protein expression, Hepatobiliary Pancreat. Dis. Int. 16 (1) (2017) 80–87.
[31] J.M. Bangen, L. Hammerich, R. Sonntag, M. Baues, U. Haas, D. Lambertz, et al., Targeting CCl4 -induced liver fibrosis by RNA interference-mediated inhibition of cyclin E1 in mice, Hepatology 66 (4) (2017) 1242–1257.
[32] J. Chen, J. Pan, J. Wang, K. Song, D. Zhu, C. Huang, et al., Soluble egg antigens of Schistosoma japonicum induce senescence in activated hepatic stellate cells by activation of the STAT3/p53/p21 pathway, Sci. Rep. 6 (2016) 30957.
[33] W. Huang da, B.T. Sherman, R.A. Lempicki, Bioinformatics enrichment tools: paths toward the comprehensive functional analysis of large gene lists, Nucleic Acids Res. 37 (1) (2009) 1–13.
[34] da W. Huang, B.T. Sherman, R.A. Lempicki, Systematic and integrative analysis of large gene lists using DAVID bioinformatics resources, Nat. Protoc. 4 (1) (2009) 44–57.